ResearchGate

See discussions, stats, and author profiles for this publication at: https://www.researchgate.net/publication/229885046

Infrared, Raman and resonance Raman investigations of methylviologen and its radical cation

ARTICLE *in* JOURNAL OF RAMAN SPECTROSCOPY · FEBRUARY 1982

Impact Factor: 2.67 · DOI: 10.1002/jrs.1250120107

CITATIONS
23

READS
44

3 AUTHORS, INCLUDING:

Martin Forster
Siemens Schweiz Zug
78 PUBLICATIONS **576** CITATIONS

SEE PROFILE

Available from: Martin Forster
Retrieved on: 24 January 2016

Infrared, Raman and Resonance Raman Investigations of Methylviologen and its Radical Cation

M. Forster†, R. B. Girling and R. E. Hester‡
Department of Chemistry, University of York, Heslington, York YO1 5DD, UK

The infrared and Raman spectra of methylviologen (1,1'-dimethyl-4,4'-bipyridine dication, MV^{2+}) have been measured from both the solid dichloride and aqueous solutions. The preresonance behaviour of MV^{2+} Raman bands showed that the absorption at ~196 nm is mainly responsible for the resonance scattering process in MV^{2+}. In the region below 1700 cm^{-1}, nine polarized ($\rho \sim 1/3$) resonance Raman bands of the methylviologen radical cation, $MV^{+\cdot}$, were assigned to in-plane ring modes. Arguments are given that the chromophore of $MV^{+\cdot}$ may also partially include the methyl groups. The excitation profiles of the $MV^{+\cdot}$ fundamentals, measured with laser wavelengths covering the range 350.6–676.4 nm, reveal three main groups of modes, each behaving differently for the excitation in this range. Modes containing largely ν(C—C) ring contributions are mainly coupled with electronic transitions at ~395, ~605 and ~720 nm and yield simple excitation profiles. Modes involving principally the vibrations of the $N^+—CH_3$ group show complicated interference peaks in the whole range of the excitation profiles. γ(CCC) is mainly coupled with the absorption at ~620 nm. Resonance Raman bands of the $(MV^{+\cdot})_2$ dimer have been characterized through studies of the concentration dependence of the spectra.

INTRODUCTION

1,1'-Dimethyl-4,4'-bipyridine dichloride, better known by the trivial names methylviologen dichloride or paraquat, is widely used as a herbicide. The herbicidal action originates from the interference of the methylviologen dication, MV^{2+}, with the respiratory system of plants. Due to its low reduction potential, $E_0(MV^{2+}/MV^{+\cdot}) = -0.44$ V, MV^{2+} by-passes the plant's chain of redox processes which ultimately should lead to CO_2 assimilation. Electrons from the primary electron acceptor of photosystem I, which should reduce ferredoxin, are intercepted by MV^{2+} and handed over to oxygen.[1]

Again due to the favourable position of its reduction potential, MV^{2+} has been used in recent years as an electron relay for the photochemical splitting of water into hydrogen and oxygen.[2–9] Several organic dyes and inorganic metal complexes when in their electronically excited states are able to reduce MV^{2+} to its radical cation $MV^{+\cdot}$.[10–17] It has been shown that $MV^{+\cdot}$ can reduce water to H_2 and OH^- at pH 7, if noble metal catalysts such as Pt/PtO_2, or colloidal Pt, are present.[2,3,18–20]

The parent compound MV^{2+} dichloride is colourless. The radical monocation $MV^{+\cdot}$ is intensely blue coloured—hence the name viologen—and shows visible absorptions which match most of the presently available laser lines. Because of the widespread interest in $MV^{2+}/MV^{+\cdot}$ and since resonance Raman (RR) spectra give much insight into the ground state vibrational structure as well as information about excited states, we found it interesting to investigate $MV^{+\cdot}$ in detail by RR spectroscopy.

In order to assign the RR bands of $MV^{+\cdot}$, the assignment of the corresponding bands of the parent compound, MV^{2+}, needs to be known. Although the Raman spectrum of MV^{2+} has been studied previously,[21] a re-examination was felt to be necessary and the new Raman data are now combined with IR data. This information has been found sufficient to interpret the RR spectra of $MV^{+\cdot}$. Excitation profiles and an overtone analysis provided further insight into the excitation process. In addition, RR bands of the $(MV^{+\cdot})_2$ dimer could be detected.

EXPERIMENTAL

Pure methylviologen dichloride from ICI Ltd was recrystallized five times from methanol/acetone.[22] Water was doubly distilled. Prepurified nitrogen was further oxygen-scrubbed by bubbling through a solution of 8 g pyrogallol and 24 g potassium hydroxide in 200 cm^3 water and was subsequently dried at 77 K. Pure zinc dust from Fisons Ltd was used to reduce MV^{2+} to the methylviologen radical cation, $MV^{+\cdot}$.

The lasers used were a Spectra Physics model 170 Kr^+, Coherent Radiation model CR4 Ar^+, and Spectra Physics model 125 HeNe. A Spex model 1403 spectrometer equipped with a cooled phototube, RCA type C31034-A02, and the Spex 1459 UVISIR sample compartment, Compudrive and Scamp minicomputers served to take the spectra.

All Raman experiments were performed using the spinning cell technique with 90° optics.[23] Removal and replacement of the kinematically mounted cell could be

† Present address: Schweizerisches Institut für Nuklearforschung, CH-5234 Villigen, Switzerland.
‡ Author to whom correspondence should be addressed.

CCC-0377-0486/82/0012-0036 $06.50

© Heyden & Son Ltd, 1982

made with almost no detectable changes in the measured intensities of resonance Raman bands. Test experiments with aqueous $KMnO_4$ solution and $\lambda_{exc} = 568.2$ nm demonstrated the repeatability of the mounting device: five experiments, involving complete removal of cell and mount in between, gave a maximum deviation from the mean count of only 2.4% for the 845 cm^{-1} band.[24] This device enabled us to measure directly the exact path length between laser focus and cell wall, which is a crucial factor for the corrections involved in calculation of excitation profiles. With the laser beam positioned at the interface between cell wall and solution, a brighter light scattering was observed, which allowed us to determine the position $d = 0$. The cylindrical cells were made from precision bore silica tubes with ϕ 35 mm (Specac Ltd, England). The focused laser beam diameter was ~3–5 μm (calculated according to Ref. 25). The distance d from the beam centre to the cell wall was 0.2 mm for most experiments. Although this value is too large for optimum intensities, the error for the determination of this distance could thus be reduced to a maximum of 5%.

For the Raman spectra of MV^{2+}, air-saturated aqueous solutions of 0.1 M MV^{2+} + 0.1 M K_2SO_4 (for preresonance investigations) or 1 M MV^{2+} (for depolarization ratios) were used. Solutions of $MV^{+\cdot}$ were prepared by filling the Raman cell with ~8 cm^3 of an aqueous solution of $3\text{–}4\times10^{-4}$ M MV^{2+} + 0.5 M K_2SO_4 at pH 7.0. This solution was then N_2-purged for 10 min, 10 mg Zn dust added and further purged for 5 min. The cell was then sealed with a Teflon stopper. After ~24 h the reduction was complete, yielding solutions with $[MV^{+\cdot}] = 1\text{–}4\times10^{-4}$ M. For spectra of higher concentrations of $MV^{+\cdot}$, aqueous solutions of $[MV^{2+}] = 3\times10^{-3}$ M, $[K_2SO_4] = 0.5$ M were used. Aqueous solutions saturated with $MV^{+\cdot}$ were obtained by Zn-reduction of aqueous 0.1 M solutions of MV^{2+}. These solutions were reddish-blue, as described in Ref. 22.

Zn particles, which were still present in the Raman cell after the reduction, had to be prevented from entering into the measuring zone. This was accomplished by first inverting the cell and its mount before starting to spin it. Spinning the cell then caused the Zn dust to be fixed in the lower part of the cell due to the centrifugal force. Still spinning, the cell and mount was then turned by 180° and fixed within the cell compartment, thus leaving the now lower part of the cell free from any particles. From VIS spectra before and after every experiment, the average $MV^{+\cdot}$ concentration was determined, using $\varepsilon(MV^{+\cdot}, 602\text{ nm}) = 1.1\times10^4$ M^{-1} cm^{-1}.[22] $MV^{+\cdot}$ decayed by ~3% during the running of a 1 h spectrum.

All Raman and resonance Raman spectra given in this work were corrected for the spectrometer sensitivity which was determined using a standard calibration lamp, Optronic-236.

Except for the RR spectra of the $(MV^{+\cdot})_2$ dimer, the spectral resolution of the monochromator was set to 5 cm^{-1} at $\Delta\nu = 0$ cm^{-1} for all excitation wavelengths. Dwell times Δt of 1 s and wavenumber steps of 1 or 2 cm^{-1} were generally used. For the $MV^{+\cdot}$ dimer spectra, the spectral resolution was 2.5 cm^{-1}, and steps of 1 cm^{-1} and Δt up to 5 s were used. Due to high absorption, the latter spectra were taken with 90° optics and grazing incidence. The depolarization ratios were corrected using CCl_4 as a reference.

UV/VIS spectra were taken either on a Unicam SP-8000 or Perkin Elmer 554 UV/VIS spectrometer.

IR spectra of MV^{2+} were taken from KBr discs on a Perkin Elmer model 580 spectrometer. The backgrounds of the digitized spectra were artificially flattened and the peaks were determined numerically from spectra smoothed by a seven-point parabola.[26]

RESULTS

Methylviologen dication, MV^{2+}

Figure 1 shows the UV absorption spectrum of MV^{2+}. Figure 2 presents the Raman spectra of MV^{2+} dichloride solid and aqueous solution. The spectra are presented here since a corresponding spectrum in the literature[21] shows additional bands which are absent from our spectra and which are also absent from the list of frequencies in Ref. 21. Table 1 contains the observed IR and Raman bands of MV^{2+} with tentative assignments.

The Raman spectra of MV^{2+} were taken with $\lambda_{exc} = 350.6$, 406.7, 476.2, 530.9 and 647.1 nm. For the construction of excitation profiles, the peak intensities were corrected by the use of the following relationships (1) and (2):

$$I_{corr}(\tilde{\nu}_{exc}) = \frac{I_s(\tilde{\nu}_s)\cdot S(\tilde{\nu}_r)\cdot \tilde{\nu}_r^4\cdot C_r\cdot 10^{(\varepsilon(\tilde{\nu}_r)+\varepsilon(\tilde{\nu}_s))}\cdot C_s\cdot d}{I_r(\tilde{\nu}_r)\cdot S(\tilde{\nu}_s)\cdot \tilde{\nu}_s^4\cdot C_s} \quad (1)$$

$$\tilde{\nu}_{s,r} = \tilde{\nu}_{exc} - \Delta\tilde{\nu}_{s,r} \quad (2)$$

$I_s(\tilde{\nu}_s)$, $I_r(\tilde{\nu}_r)$ are the observed signal peak heights of sample s and reference r at $\tilde{\nu}_s$, $\tilde{\nu}_r$, respectively. $\tilde{\nu}_{exc}$ is the laser excitation wavenumber and $\Delta\tilde{\nu}_{s,r}$ the Raman wavenumber of the sample or the reference, respectively. $S(\tilde{\nu}_{r,s})$ are the relative sensitivities of the system

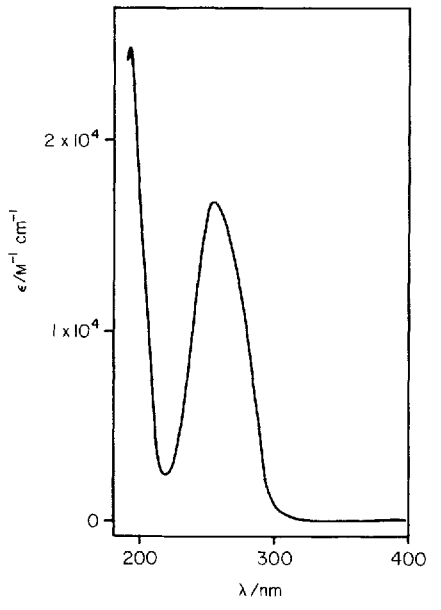

Figure 1. Absorption spectrum of 7×10^{-5} M methylviologen dichloride in H_2O at 25 °C.

© Heyden & Son Ltd, 1982

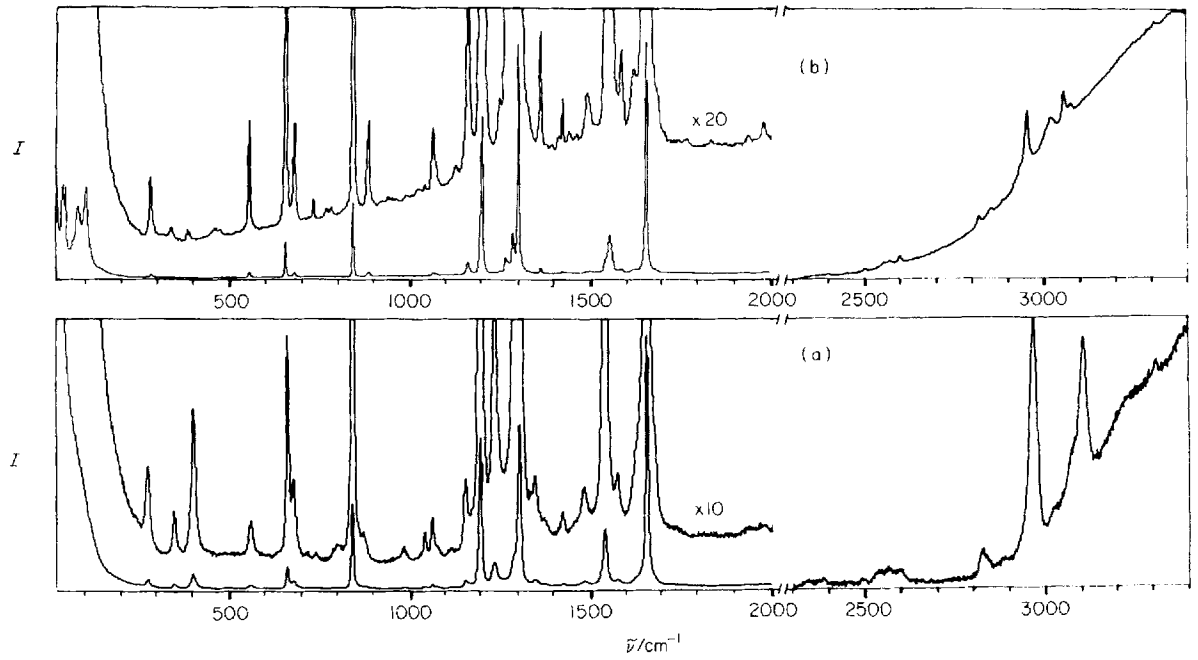

Figure 2. Raman spectra of methylviologen dichloride, (a) 1 M in H_2O, (b) solid. $\lambda_{exc} = 476.2$ nm, spectral slit width 5 cm^{-1} for solution, 2.5 cm^{-1} for solid.

monochromator plus photomultiplier at $\tilde{\nu}_{r,s}$. C_r, C_s are the concentrations of the reference, K_2SO_4, and the sample, MV^{2+}, in mol dm^{-3}, respectively. $\varepsilon(\tilde{\nu}_{r,s})$ are the molar decadic absorption coefficients of MV^{2+} at $\tilde{\nu}_{r,s}$ and d is the distance from the focused laser beam centre to the cell wall. For a system where only one excited state is dominant in the resonance Raman effect, the intensity of a Raman band in the preresonance region is governed by the Albrecht-Hutley factor $F_A^2(\tilde{\nu}_s)$:[27]

$$F_A^2(\tilde{\nu}_s) = \frac{\tilde{\nu}_s^4(\tilde{\nu}_e^2 + \tilde{\nu}_{exc}^2)^2}{(\tilde{\nu}_e^2 - \tilde{\nu}_{exc}^2)^4} \quad (3)$$

$\tilde{\nu}_e$ is the wavenumber of the electronic transition from ground to excited state. For the case where two excited states are important for the scattering process, the scattered intensity is proportional to

$$F_B^2(\tilde{\nu}_s) = \frac{4\tilde{\nu}_s^4(\tilde{\nu}_{e1}\tilde{\nu}_{e2} + \tilde{\nu}_{exc}^2)^2}{(\tilde{\nu}_{e1}^2 - \tilde{\nu}_{exc}^2)^2(\tilde{\nu}_{e2}^2 - \tilde{\nu}_{exc}^2)^2} \quad (4)$$

Here $\tilde{\nu}_{e1}$ and $\tilde{\nu}_{e2}$ are wavenumbers for transitions to two different excited states. In this work, normalized values of $A(\tilde{\nu}_{exc})$ and $B(\tilde{\nu}_{exc})$ were used, according to Eqn (5):

$$A(\tilde{\nu}_{exc}) = \frac{F_A^2(\tilde{\nu}_s) \cdot \tilde{\nu}_n^4}{F_A^2(\tilde{\nu}_n) \cdot \tilde{\nu}_s^4} \quad (5)$$

and similarly for $B(\tilde{\nu}_s)$, with $\tilde{\nu}_n$ being the excitation wavenumber selected for normalization. $A(\tilde{\nu}_{exc})$, $B(\tilde{\nu}_{exc})$ are now independent of the Raman frequencies $\Delta\tilde{\nu}_s$ and no longer contain the $\tilde{\nu}_s^4$ dependence. Therefore, without any preresonance effect, the terms $A(\tilde{\nu}_{exc})$ and $B(\tilde{\nu}_{exc})$ would be unity for all excitation wavenumbers $\tilde{\nu}_{exc}$.

The observed values of $I_{obs}(\tilde{\nu}_{exc})$,

$$I_{obs}(\tilde{\nu}_{exc}) = I_{corr}(\tilde{\nu}_{exc})/I_{corr}(\tilde{\nu}_n) \quad (6)$$

can now be compared with either $A(\tilde{\nu}_{exc})$ or $B(\tilde{\nu}_{exc})$ for different $\tilde{\nu}_{e1}$, $\tilde{\nu}_{e2}$ in order to determine which of the excited states takes part in the resonance Raman process.

Table 2 compares the theoretical values of $A(\tilde{\nu}_{exc})$ and $B(\tilde{\nu}_{exc})$ for the UV transitions at 39 216 and 52 083 cm^{-1} with the experimental values of $I_{obs}(\tilde{\nu}_{exc})$.

Methylviologen radical cation, $MV^{+\cdot}$

The RR spectra of $MV^{+\cdot}$ in H_2O have been measured at eleven excitation wavelengths: 350.6, 406.7, 413.1, 457.9, 476.8, 488.0, 514.5, 530.9, 632.8, 647.1 and 676.4 nm. The spectra were taken with dilute solutions ($0.7–3.9 \times 10^{-4}$ M) and with concentrated ones ($\sim 3 \times 10^{-3}$ M). $MV^{+\cdot}$ is known to dimerize in aqueous solution at room temperature—the dissociation constant K for the reaction $[D] \rightleftarrows 2\,MV^{+\cdot}$ is $K = 2.6 \times 10^{-3}$ M.[22,28] The dilute solutions had maximal ratios [D]/[M] = 0.1 and the concentrated ones [D]/[M] $\approx$ 0.55.

Figure 3 shows the RR spectra of dilute solutions of $MV^{+\cdot}$ in the range 200–1800 cm^{-1} with $\lambda_{exc} = 350.6$ to 676.4 nm. Drastic changes in intensity of the RR bands between the spectra are obvious.

Figure 4 shows the RR overtones and combination bands of $MV^{+\cdot}$ for $\lambda_{exc} = 568.2$ and 350.6 nm.

A better insight into the frequency dependence of the RR intensities is given by Fig. 5, which contains the excitation profiles of all the fundamental RR bands of $MV^{+\cdot}$ that are listed in Table 3. The depolarization ratios of all the bands in Table 3, measured with $\lambda_{exc} =$ 514.5 nm, lie between 0.28 and 0.39.

Figure 5 contains also the absorption spectrum of $MV^{+\cdot}$. The part in the visible region and centred at ~605 nm could be resolved into six Gaussian components, using a modified band deconvolution program due to R. N. Jones.[32] The parameters of this fit are listed in Table 4.

In Fig. 6 the appearance of overtones and combination bands of $MV^{+\cdot}$ with different λ_{exc} is given. The long

© Heyden & Son Ltd, 1982

Table 1. IR and Raman band wavenumbers/cm^{-1} and tentative assignments for methylviologen dichloride

IR[a] (solid)	Raman[b] (solid)	Raman[c] (solution)	Assignment[d]	IR[a] (solid)	Raman[b] (solid)	Raman[c] (solution)	Assignment[d]
	3310 vw	3307 vw, p	2×1655	1269 w			
		3105 w, p			1264 vw		
	3074 vw	3074 vw, sh, p		1254 w	1248 vw		
3052 w	3055 vw			1235 s	1242 vw	1234 w, p	Ring
		3036 vw, sh,		1229 w			
		dp	ν(C—H)	1205 w	1200 s		
3018 w	3107 vw				1194 w	1193 s, p	Ring
2994 w				1181 s			+ν(N$^+$—CH$_3$)
2965 w		2967 w, p			1160 w	1152 vw, dp	
	2954 vw			1136 vw			
	2935 vw		ν(CH$_3$)	1126 m	1126 vw		
		2880 vw, p		1109 vw		1113 vw, p	
2856 w	2853 vw			1074 w			
	2820 vw	2828 vw, p			1061 vw	1061 vw, p	
	2601 vw	2600 vw, p	2×1300	1055 w			
	2573 vw	2569 vw, p		1039 vw	1041 vw	1040 vw, dp	γ(CH$_3$)
		2540 vw, p			1021 vw		
	2504 vw			993 vw			
	2401 vw					982 vw, p	
		2386 vw, p		959 m			
	2355 vw		Overtones		939 vw		
		2344 vw	and		886 vw		
	2233 vw	2230 vw	combination		882 vw	872 vw, dp	
	1980 vw	1977 vw	bands	846 m	843 m	841 m, p	Ring
	1938 vw	1937 vw				795 vw, p	+ν(N$^+$—CH$_3$)
	1834 vw			786 m	782 vw		+γ(C—N$^+$—CH$_3$)
	1766 vw			766 m	768 vw		
	1685 vw, sh			757 m			
	1676 vw, sh	1679 vw, sh		733 vw	732 vw	739 vw, p	
	1654 vs	1654 vs, p				714 vw, dp	
1640 s				706 m			
	1618 vw	1621 vw, sh			679 vw	676 vw, p	
1594 vw				672 w			
	1585 vw	1573 vw, p		669 vw			
1562 m					656 w	660 w, p	Ring
	1552 w			622 vw			+γ(C—N$^+$—CH$_3$)
	1540 vw, sh	1538 m, p			555 vw	558 vw, p	
1508 m				537 vw			
	1491 vw	1480 vw, p			475 vw		
1461 m				469 s			
1440 m	1440 vw		δ(CH$_3$)$_{as}$		463 vw		
	1422 vw	1422 vw, p		404 vw			
	1411 vw			393 w	390 vw	398 w, p	
1392 w	1392 vw				384 vw		
1384 w					340 vw	345 vw, dp	Ring
	1361 m	1371 vw, p	δ(CH$_3$)$_{sym}$		281 vw	271 vw, p	
1356 m					101 w		
		1345 vw, dp			79 w		
1324 w					65 vw		Lattice
	1301 vs	1301 s, p	ν(C—C)$_{i.r.}$		44 w		modes
	1286 w	1285 vw, sh, dp			38 m		
	1273 vw				34 w		

[a] KBr pellet.
[b] Pure $MV^{2+}Cl_2^{2-}$, $\lambda_{exc} = 476.2$ nm.
[c] 1 M in H_2O, $\lambda_{exc} = 476.2$ nm.
[d] Refs 21, 29, 38–42.
s = strong, m = medium, w = weak, v = very, p = polarized, dp = depolarized, sh = shoulder.
ν = stretching mode, γ = in-plane bending, δ = out-of-plane bending, i.r. = inter-ring, sym = symmetric, as = asymmetric.

bars indicate the appearance of the overtones even in dilute solutions with the corresponding excitation wavelength, short bars the appearance only in concentrated solutions. Figure 6 represents, therefore, the qualitative excitation profiles of these bands. For the combination bands 2348 and 2560 cm^{-1}, quantitative

© Heyden & Son Ltd, 1982

Table 2. Theoretical $A(\tilde{\nu}_{exc})$ and $B(\tilde{\nu}_{exc})$[a] and experimental $I_{obs}(\tilde{\nu}_{exc})$[a] for the preresonance behaviour of prominent Raman bands of MV^{2+} in H_2O[b]

		$A(\tilde{\nu}_{exc})$ theor.[c]		$B(\tilde{\nu}_{exc})$ theor.[d]	$I_{obs}(\tilde{\nu}_{exc})$ at $\Delta\tilde{\nu}/cm^{-1}$					
λ_{exc}/nm	$\tilde{\nu}_{exc}/cm^{-1}$	$\tilde{\nu}_e = 39\,216\ cm^{-1}$	$\tilde{\nu}_e = 52\,083\ cm^{-1}$	with $\tilde{\nu}_{e1}$ and $\tilde{\nu}_{e2}$	660	841	1193	1301	1538	1654
647.1	15 449	0.41	0.62	0.51	0.77	0.85	0.64	0.61	0.61	0.59
530.9	18 832	0.68	0.82	0.74	0.92	0.95	0.85	0.81	0.71	0.77
476.2	20 992	1.00	1.00	1.00	1.00	1.00	1.00	1.00	1.00	1.00
406.7	24 588	2.24	1.49	1.82	1.54	1.48	1.80	1.59	1.67	1.76
350.6	28 523	7.44	2.56	4.34	2.82	2.47	4.02	3.56	3.68	4.11

[a] Using 20 992 cm^{-1} as the normalizing wavenumber $\tilde{\nu}_n$ in Eqn (5).
[b] 0.1 M methylviologen dichloride and 0.1 M K_2SO_4 in H_2O.
[c] Calculated according to Eqn (3).
[d] Calculated according to Eqn (4) with $\tilde{\nu}_{e1} = 39\,216\ cm^{-1}$, $\tilde{\nu}_{e2} = 52\,083\ cm^{-1}$.

excitation profiles are also included in Fig. 5. Table 5 contains additional high frequency bands, which were observed only with $\lambda_{exc} = 350.6$ nm.

Figures 7 and 8 give information about the concentration dependence of the RR spectra of $MV^{+\cdot}$. In Fig. 7 the fundamental region of $MV^{+\cdot}$ is compared for dilute and concentrated solutions. Obviously some intensity changes occur for the fundamentals at 1028 and 1534 cm^{-1} by going from low to high concentration. Furthermore, bands at 664, 1028, 1188, 1340, 1512 and 1604 cm^{-1} become more intense for the concentrated solution. A similar behaviour, but not so clearly recognizable, was observed for $\lambda_{exc} = 413.1$, 476.8, 488.0, 514.5, 530.9 nm. In Fig. 8 the combination bands at 2538 and 2560 cm^{-1} for $\lambda_{exc} = 488.0$ and 514.5 nm are compared for dilute and concentrated solutions. For $350.6 \leq \lambda_{exc}/nm < 488.0$ no combination bands around 2550 cm^{-1} were observed for dilute solutions and for $\lambda_{exc} \geq 514.5$ nm no difference between concentrated and dilute solutions could be seen.

The depolarization ratios of the bands at 1340 and 1512 cm^{-1} were measured with saturated aqueous $MV^{+\cdot}$ solution. Interestingly, these bands are found to be fully depolarized and may even show slight inverse polarization ($\rho \sim 0.9$), although band overlap makes this measurement prone to rather larger error than normal.

DISCUSSION

Methylviologen dication, MV^{2+}

Molecular structure. According to X-ray analysis, the methylviologen dication MV^{2+} has the two rings coplanar in the solid form,[33] but no information about

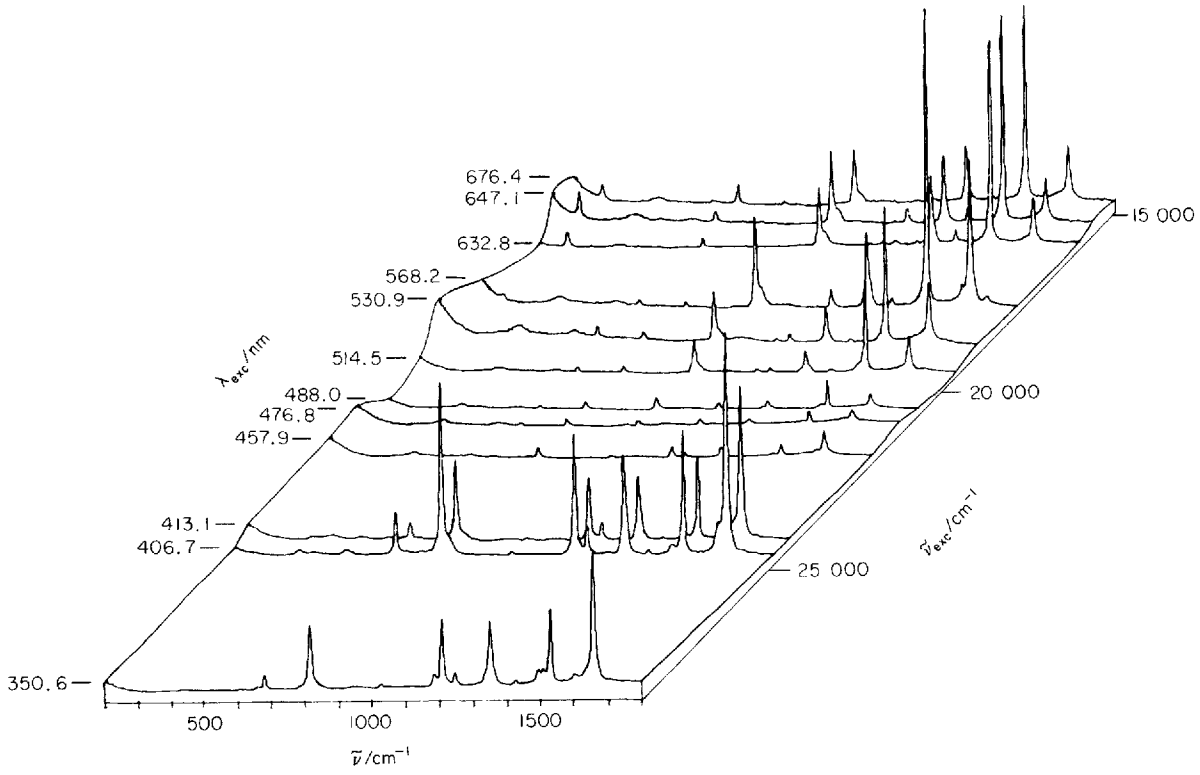

Figure 3. RR spectra of $0.7–3.9 \times 10^{-4}$ M $MV^{+\cdot}$ in H_2O with different excitation wavelengths λ_{exc}, intensities normalized for constant concentration, SO_4^{2-} bands removed.

© Heyden & Son Ltd, 1982

Table 3. RR active fundamentals of $MV^{+\cdot}$ in H_2O, compared with MV^{2+}, BP[a] and $BP^{-\cdot}$,[b] and tentative assignments

Potential energy distribution for BP[c]	λ_{exc} = 632.8 nm			λ_{exc} = 514.5 nm			Assignments[g]
	BP^{d}/cm^{-1}	$BP^{-\cdot e}/cm^{-1}$	Δ^{f}/cm^{-1}	MV^{2+}/cm^{-1}	$MV^{+\cdot}/cm^{-1}$	Δ^{f}/cm^{-1}	
ν(CH)98	3080	—	—	3105	—	—	
ν(CH)98	3073	—	—	3074	—	—	
	—	—	—	2967	—	—	$\nu(CH_3)_s$
ν(CC)66, $\nu(CC)_{i.r.}$11, γ(CCH)29	1605	1587	−18	1654 p	1662 p	+8	
ν(CC)40, γ(CCH)45	1510	1493	−17	1538 p	1534 p	−4	
				1371 p	1430 p	+59	$\delta(CH_3)_s$ in-phase
ν(CC)12, $\nu(CC)_{i.r.}$43, γ(CCC)10	1287	1326	+39	1301 p	1356 p	+55	ν(C—C) inter-ring
γ(CCH)21		1250		1234 p	1250 p	+16	
ν(CC)19, γ(CCH)68	1190	1201	+11	1193 p	1212 p	+19	$+\nu(N^{\cdot}—CH_3)$
					1046 sh		
ν(CC)46, γ(CCC)16, γ(CCH)18	1033	1017	−16	1061 p	1028 p	−33	
ν(CC)57, γ(CCC)17	1005	979	−26	841 p	818 p	−23	$+\nu(N^{+}—CH_3)+\gamma(C—N^{+}—CH_3)$
ν(CC)22, γ(CCC)46, γ(CCH)12	743	721	−22	660 p	682 p	+22	$+\gamma(C—N^{+}—CH_3)$
ν(CC)11, $\nu(CC)_{i.r.}$30, γ(CCC)40	314	327	+13	271 p	282 p	+11	

[a,b] BP, $BP^{-\cdot}$ = biphenyl, biphenyl radical anion, respectively.
[c] in %, only values ≧10% noted, similar modes added together (Ref. 29).
[d] Refs 30, 40.
[e] Refs 30, 31.
[f] $\Delta = \tilde{\mu}(BP^{-\cdot}) - \tilde{\nu}(BP)$ or $\tilde{\nu}(MV^{+\cdot}) - \tilde{\nu}(MV^{2+})$.
[g] Only information additional to the PED of BP is given.
ν = stretching, γ = in-plane bending, δ = out-of-plane bending, p = polarized, s = symmetric, i.r. = inter-ring, sh = shoulder.

the positioning of the methyl groups is available. Since toluene has a barrier height for the internal rotation of the methyl group of 840 J mol^{-1} in the crystalline state,[34] an almost free rotation of the methyl group in liquid toluene at room temperature has been postulated.[35] Even for solid hexamethylbenzene at room

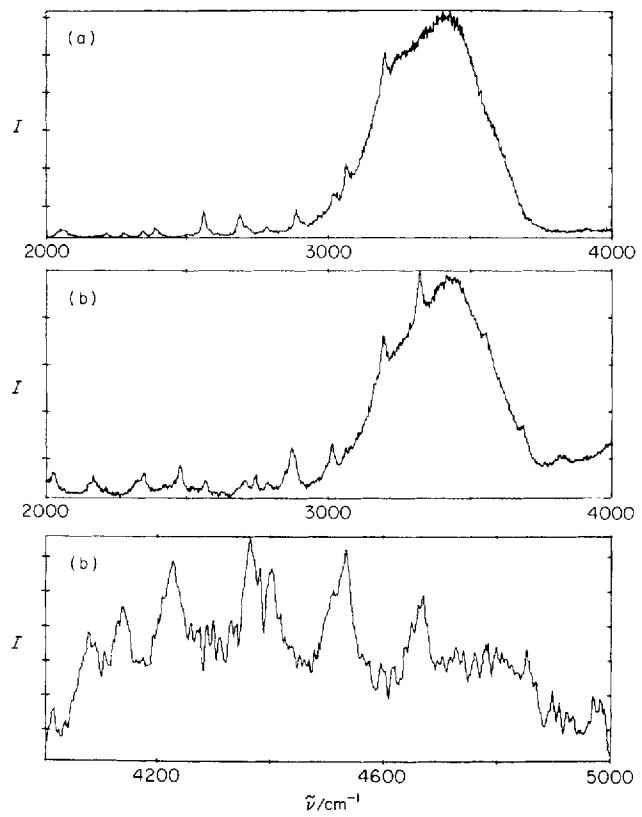

Figure 4. RR spectra of $MV^{+\cdot}$ with 0.5 M K_2SO_4 in H_2O, overtones and combination bands, λ_{exc} = 568.2 nm (a), 350.6 nm (b).

Table 4. Bandshape analysis of the VIS absorption spectrum of $MV^{+\cdot}$ in aqueous solution[a,c]

Band number	$\tilde{\nu}_0$[b]/cm^{-1}	λ[b]/nm	Width at half height/cm^{-1}	Relative intensity
1	19 185	521	2430	0.22
2	17 554	570	1984	0.67
3	16 440	608	1100	0.62
4	15 820	632	753	0.27
5	14 991	667	1313	0.43
6	13 619	734	646	0.14

[a] ~1×10^{-4} M $MV^{+\cdot}$ at room temperature.
[b] Centre wavenumber and wavelength, respectively.
[c] No improvement in the resolution of the spectra was obtained from $MV^{+\cdot}$ produced at 77 K by UV irradiation of 1×10^{-3} M MV^{2+} dichloride in EtOH.

Table 5. Overtones and combination bands for 3.4×10^{-4} M $MV^{+\cdot}$ in H_2O, observed only with λ_{exc} = 350.6 nm

$\tilde{\nu}$/cm^{-1}	Fundamental composition
3556	682 + 1212 + 1662 = 3556
3688	818 + 1212 + 1662 = 3692
3824	818 + 1356 + 1662 = 3836
4016	818 + 1534 + 1662 = 4014
4086	1212 + 1212 + 1662 = 4086
4140	818 + 1662 + 1662 = 4142
4226	1212 + 1356 + 1662 = 4228
4366	1356 + 1356 + 1662 = 4374
4400	1212 + 1534 + 1662 = 4408
4534	1212 + 1662 + 1662 = 4536
4668	1356 + 1662 + 1662 = 4680
4858	1534 + 1662 + 1662 = 4858
4984	1662 + 1662 + 1662 = 4986

© Heyden & Son Ltd, 1982

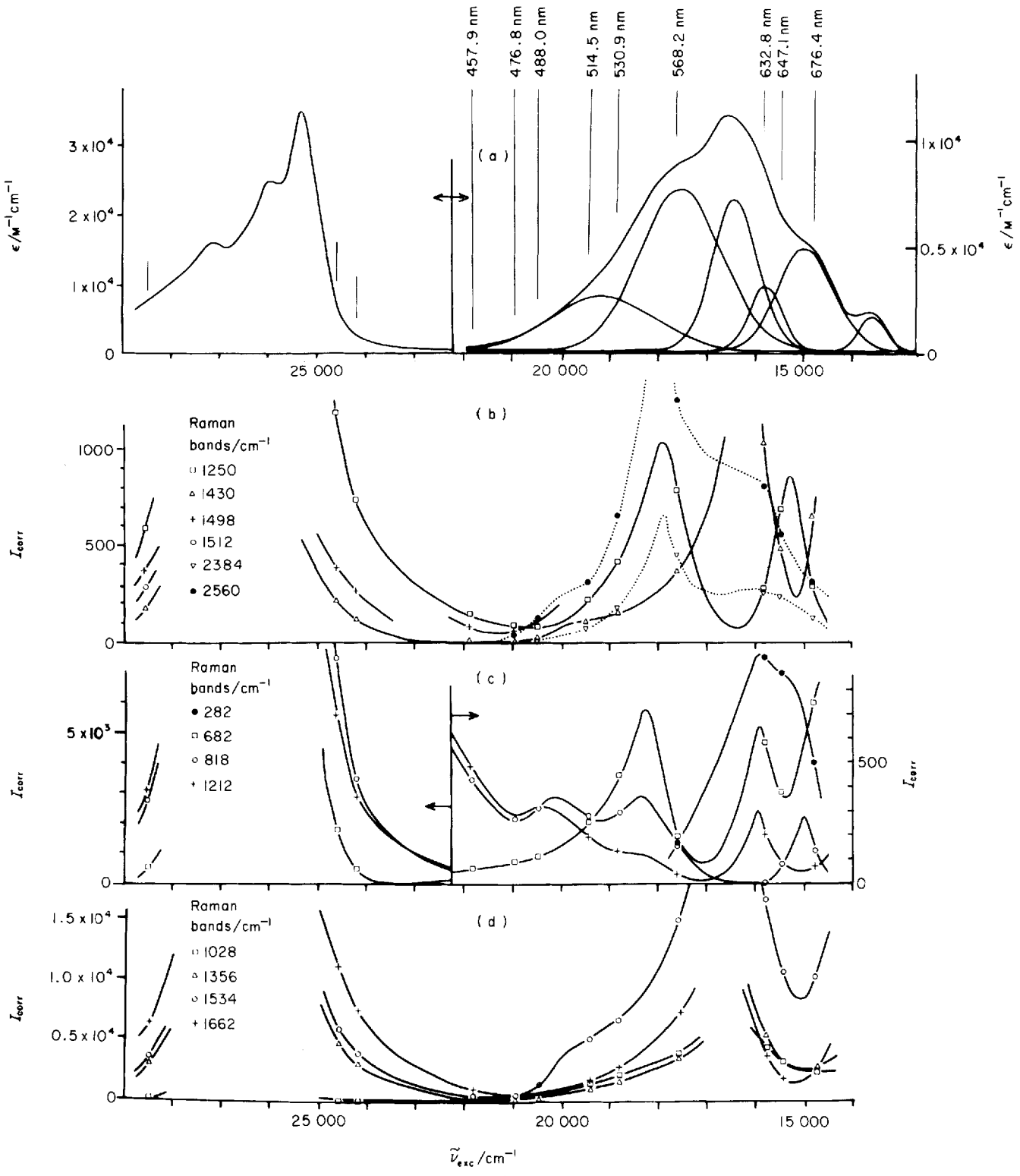

Figure 5. Excitation profiles of RR bands of 0.7–3.9 × 10 $^{-4}$ M $MV^{+\cdot}$ in H_2O and VIS absorption spectrum of $MV^{+\cdot}$ with bandshape analysis.

temperature, almost free rotation of the methyl groups has been found.[36] We assume, therefore, free rotation of the methyl groups in solid MV^{2+} as well. With D_{2h} symmetry overall and C_{3v} local symmetry for the methyl groups, the IR and Raman frequencies of the rings should be mutually exclusive, but for the methyl groups they should coincide. From the eleven coincidences between IR and Raman bands in Table 1 for solid MV^{2+}, at least two (2856/2853 and 1440/1440 cm^{-1}) can be ascribed to the CH_3 groups. The other nine coincidences might be accidental or due to closely related, in-phase (Raman) and out-of-phase (IR)

© Heyden & Son Ltd, 1982

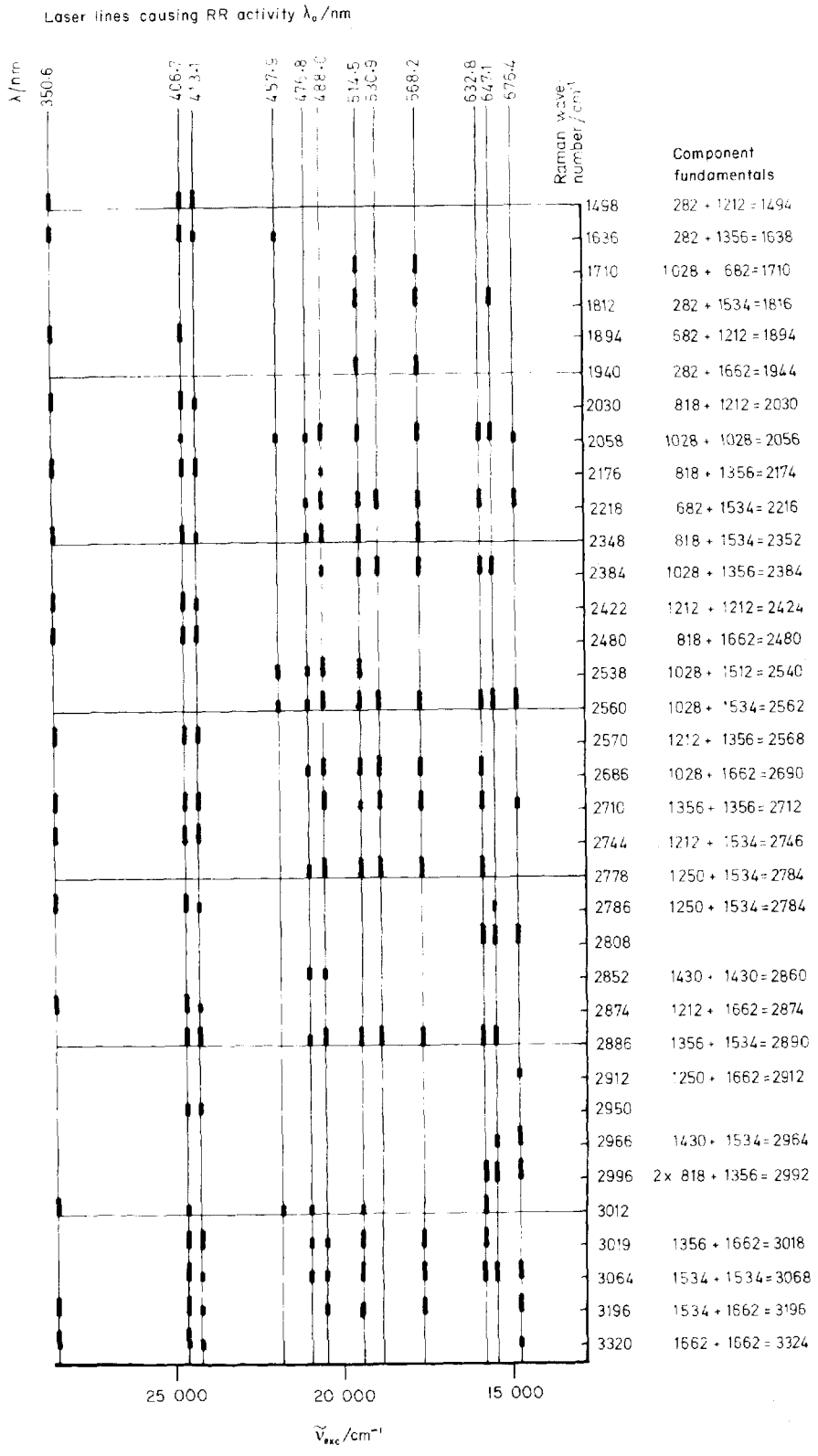

Figure 6. RR activities of overtones and combination tones of $MV^{+\cdot}$ in H_2O. The shorter markers indicate appearance only in spectra from concentrated solution ($\sim 3 \times 10^{-3}$ M). Otherwise appearance in dilute solutions ($0.7–3.9 \times 10^{-4}$ M $MV^{+\cdot}$).

modes, as has been calculated and measured for 4,4'-dihalogenobiphenyls.[37]

Table 1 and Fig. 2 show that the Raman spectra from solution differ mainly in the ν(CH) region from those of the solid. In total, 9 bands of the solution spectrum had no counterpart in the solid spectrum and 22 bands of the solid had no counterpart for the solution spectrum (lattice modes and combination tones excluded).

© Heyden & Son Ltd, 1982

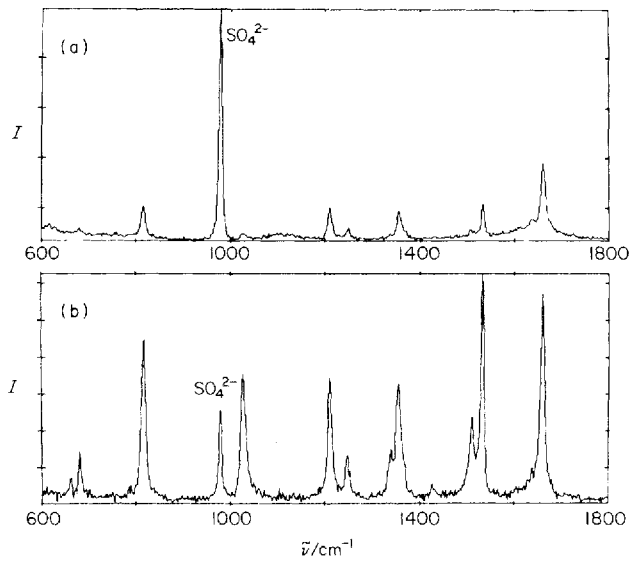

Figure 7. Effects of concentration changes on the RR fundamentals of the spectrum of $MV^{+\cdot}$ in H_2O with $\lambda_{exc} = 457.9$ nm. (a) 1.4×10^{-4} M $MV^{+\cdot}$, (b) $\sim 3 \times 10^{-3}$ M $MV^{+\cdot}$.

Although the higher number of bands detected for the solid can partially be explained by the very high signal-to-noise ratio of this spectrum ($S/N \approx 4 \times 10^3$ for the most intense bands), the high number of polarized Raman bands in solution also indicates a lowering of symmetry for the ring when going from solid to solution.

The CH_3 groups are again assumed to be freely rotating, as was observed for *N*-methyl pyridinium chloride in water.[38] If no coupling is assumed between the two CH_3 groups, 14 polarized and 21 depolarized Raman and 32 IR bands would be expected for coplanar rings (D_{2h} symmetry). For twisted rings (twist angle $0 < \phi < 90°$, symmetry D_2) the expected numbers are 21, 45 and 48, respectively. Subtracting the obvious overtones and combination bands, we observe 24 polarized and 8 depolarized Raman lines.

Depolarized bands can easily escape detection and, since some of the assumed polarized fundamentals can turn out to be combination bands, symmetry D_2 seems to be appropriate for MV^{2+} in solution. This is in contrast to Ref. 21 but agrees with Ref. 37 where a similarly twisted structure was found for 4,4'-dihalogenodiphenyls.

Band assignment. Since no isotopic data are available, the tentative band assignments in Table 1 were made by using literature data[21,39] and by comparison with similar molecules, like biphenyl[29,40–42] and *N*-methyl pyridinium chloride.[38] Only those assignments are given in Table 1 which could be made without ambiguity. The polarized Raman bands at 1301, 1193 and 841 cm^{-1} could be assigned to the ν(C—C) inter-ring mode, by comparison with biphenyl,[29] and to in-plane ring modes with contributions from $\nu(N^+—CH_3)$ as in *N*-methyl pyridinium chloride.[38]

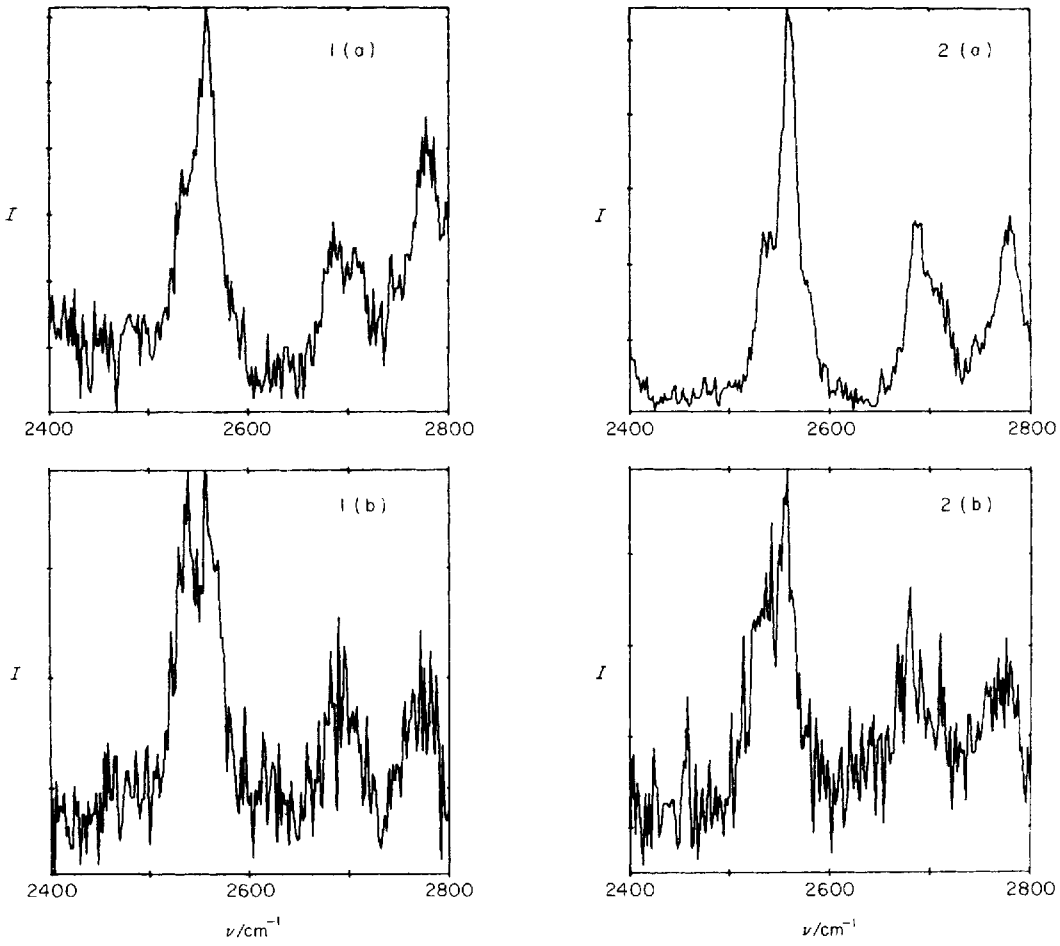

Figure 8. Effects of concentration changes on the combination bands of the RR spectrum of $MV^{+\cdot}$ in H_2O with $\lambda_{exc} = 488.0$ (1), 514.5 nm (2). (a) $1.6–1.7 \times 10^{-4}$ M, (b) $\sim 3 \times 10^{-3}$ M $MV^{+\cdot}$.

© Heyden & Son Ltd, 1982

The results of a normal coordinate analysis for the totally symmetric modes of biphenyl,[29] which is isoelectronic with the ring system of MV^{2+}, is compared in Table 3 with the totally symmetric modes of MV^{2+}. A satisfactory correlation between the two sets of modes could be achieved. The main discrepancies lie in the low frequency region, where the mixing of the in-plane bending $\gamma(C-N^+-CH_3)$ probably leads to large changes in the vibrational frequencies. Table 3 also shows the potential energy distribution of the biphenyl modes which will, as a rough approximation, also describe the mode composition of MV^{2+}.

For MV^{2+} in the solid state, the weak shoulders at 1540 and 1194 cm^{-1} of the Raman bands at 1552 and 1200 cm^{-1}, respectively, are possibly due to site splitting.

Preresonance enhancement of MV^{2+} Raman lines. Methylviologen dichloride absorbs in the UV at 258 and 196 nm ($\tilde{\nu}_{e1} = 39\,216$, $\tilde{\nu}_{e2} = 52\,083$ cm^{-1}, respectively). By varying the excitation from 15 449 cm^{-1} (647.1 nm) to 28 523 cm^{-1} (350.6 nm) a considerable preresonance effect should occur. As Table 2 shows, this is indeed the case. But the observed intensity values, $I_{obs}(\tilde{\nu}_{exc})$, indicate that not only the first transition at $\tilde{\nu}_{e1}$ is involved in the scattering process. For the bands at 660 and 841 cm^{-1} the second transition, $\tilde{\nu}_{e2}$, alone can account for the results. For the remaining bands at 1193, 1301, 1538 and 1654 cm^{-1} the transitions at $\tilde{\nu}_{e1}$ and $\tilde{\nu}_{e2}$ (*B*-term) are both relevant for the scattering process. These results suggest, as with the findings for *p*-nitroaniline,[27] that during excitation to the first excited singlet state at 258 nm, only small structural changes occur along the normal coordinates with wavenumbers of 660 and 841 cm^{-1}. These normal modes couple with the higher energy transition at 196 nm or at even shorter wavelengths. The remaining normal modes given in Table 2 evidently couple with the transition at 258 nm as well as at 196 nm. The different behaviour of the bands at 660 and 841 cm^{-1} probably originates from considerable contributions of the in-plane bending, $\gamma(C-N^+-CH_3)$ (see Table 3), which is absent from the other modes.

Methylviologen radical cation, $MV^{+\cdot}$

UV/VIS absorption spectrum. $MV^{+\cdot}$ shows three main absorption bands[22] centred at ~250, ~395 and 605 nm. This spectrum is strikingly similar to those of both the 2,2′-pipyridyl, $Bpy^{-\cdot}$,[43] and the biphenyl, $BP^{-\cdot}$,[44] radical anions. The aromatic rings of $MV^{+\cdot}$, $Bpy^{-\cdot}$ and $BP^{-\cdot}$ are isoelectronic and since both $Bpy^{-\cdot}$[45] and $BP^{-\cdot}$[46] are known to be planar, we also make this assumption of planarity for $MV^{+\cdot}$. To our knowledge the only theoretical work on the UV/VIS spectrum of $MV^{+\cdot}$ is a semi-empirical PPP calculation.[47] Since the π-systems of $MV^{+\cdot}$ and $BP^{-\cdot}$ are isoelectronic, we therefore used the results of a PPP–SCF-MO-CI calculation of the $BP^{-\cdot}$ absorption[46] to interpret the $MV^{+\cdot}$ spectrum. According to Ref. 46 the transition which gives rise to the absorption at 585 nm[44] in $BP^{-\cdot}$ occurs between the molecular orbitals with symmetries B_{3u} and B_{2g}, respectively. As Fig. 5 and Table 4 show, the absorption band for this theoretically predicted single transition could be resolved into at least six Gaussian components. This structure presumably has a vibronic origin, but no regular spacing of the centre frequencies of these components is observed which could be attributed to one dominant mode in the vibronic structure.

Resonance Raman spectra of dilute $MV^{+\cdot}$ solutions

Fundamentals and tentative assignments. The decision as to which of the observed RR bands of $MV^{+\cdot}$ are fundamentals was made in the following way:

(i) all those bands which showed enhanced relative intensity when going from dilute to concentrated solutions were discarded as due to dimers;
(ii) all the frequencies which could be explained satisfactorily as a sum of other observed frequencies were also discarded;
(iii) frequencies which occurred as components in overtones or combination tones were assumed to be fundamentals.

Using this method, the only ambiguity occurred with the shoulder at 1046 cm^{-1}, which did not fulfil criterion (iii). All other bands listed in Table 3 are believed to be fundamentals of $MV^{+\cdot}$.

With two exceptions, the correlation of these frequencies either with those of MV^{2+} or with the frequencies of $BP^{-\cdot}$ is straightforward. Therefore, the potential energy description of the BP modes can also be used as an approximation for $MV^{+\cdot}$. The large shift of +55 cm^{-1} in going from MV^{2+} to $MV^{+\cdot}$ for the vibration containing a large contribution from ν(C—C) inter-ring (1301 → 1356 cm^{-1}) is worthy of special comment. Similar shifts are observed for the pair BP → $BP^{-\cdot}$ (1287 → 1326 cm^{-1}) (see Table 3) and for benzidine → benzidine$^{+\cdot}$.[48] For all these radicals the inter-ring C—C bond is assumed to have a considerably increased π-bond order, which explains the increased frequency of the mode.

If only the two rings are considered, with the methyl groups as point masses, eleven totally symmetric modes of the symmetry type A_g should occur within the molecular symmetry D_{2h}. Nine of these bands should lie below 1700 cm^{-1}, with at least one mode containing a high contribution of $\nu(N^+-CH_3)$. But Table 3 shows eleven bands listed as fundamentals, including the shoulder at 1046 cm^{-1}. The latter band could be explained by Fermi resonance, yielding the pair at 1028/1046 cm^{-1}.

Of the other ten fundamentals, the one at 1430 cm^{-1} is subject to the most uncertainty. This band is correlated with the 1371 cm^{-1} MV^{2+} band which is likely to be the symmetric and in-phase $\delta(CH_3)_s$, judged from the comparison with *p*-xylene[49] or *N*-methylpyridinium chloride.[38] But this mode can only be resonance enhanced in $MV^{+\cdot}$ if the CH_3 groups also belong, at least partially, to the chromophore giving rise to the absorptions at ~395 and ~605 nm. This might indeed be possible, since the UV/VIS absorption spectra of *N*,*N*′-disubstituted-4,4′-bipyridine radical cations are slightly dependent on the alkyl substituent.[1,50] Furthermore, the large shift of +59 cm^{-1} in going from MV^{2+} to $MV^{+\cdot}$ suggests a much 'stiffer' CH_3 group for $MV^{+\cdot}$ than for MV^{2+}, indicating an enhanced electron density within the CH_3 group for $MV^{+\cdot}$. That this is indeed the case is shown by ESR spectroscopy: the unpaired

© Heyden & Son Ltd, 1982

electron is delocalized symmetrically over the whole cation from one methyl group to the other.[51]

If one accepts the assignment of the 1430 cm^{-1} $MV^{+\cdot}$ band to $\delta(CH_3)_s$, the problem with the surplus fundamental is then solved as well: nine fundamentals are then expected from the ring modes and the 1430 cm^{-1} band belongs to the CH_3 groups. Due to a high number of overtones, the other two expected ν(C—H) ring modes could not be assigned definitely in the RR spectra of $MV^{+\cdot}$. Interestingly, in Fig. 6, which shows the overtones of $MV^{+\cdot}$, three bands at 2808, 2950 and 3012 cm^{-1} could not be assigned to overtones. The first two bands could represent $\nu(CH_3)$ modes, whereas the latter could be due to a ν(C—H) mode. However, we are not confident about this assignment and a definite confirmation could be obtained only with further experiments which included deuterated $MV^{2+}/MV^{+\cdot}$.

Excitation profiles. The excitation profiles in Fig. 5, which are estimated to be correct within ±5%, show a great complexity due to interference effects. Excitation profiles of similar complexity previously have been observed only for big macrocycles like porphyrins[52–54] or phthalocyanines.[55] $MV^{+\cdot}$ seems to be the first example of a relatively small molecule with such a complicated resonance behaviour. Although the excitation profiles in Fig. 5 are taken with a wide spacing of excitation lines, they are believed to represent the gross features of the true profiles, which can be obtained only with continuously tuned dye lasers.

Without explaining the origin of each of the peaks in Fig. 5, in the following section some observations are given which might help to clarify the situation.

Four types of excitation profile can be distinguished:

Type 1 with resonance enhancements mainly at ~395, ~605 and ~720 nm. These wavelengths each correspond to UV/VIS absorption bands (see Fig. 5 and Table 4). To this group belong the bands at 1028, 1356, 1430, 1534 and 1662 cm^{-1}.

Type 2 bands show enhancement at ~395 nm and several peaks in the range 450–700 nm. To this group belong 682, 818, 1212 and 1250 cm^{-1}.

Type 3 bands peak only at ~395 nm: 1498, 1512 cm^{-1}.

Type 4 bands peak only in the range 550–650 nm: 282, 2384, 2560 cm^{-1}.

A comparison of these groups with the assignments given in Table 3 yields the following analysis. Type 1 modes contain high contributions from ν(C—C) of the rings. An exception is the band at 1430 cm^{-1}, but this also shows much less resonance enhancement than the other members of this group.

Type 2 modes contain contributions which involve the $N^+—CH_3$ group vibrations. The band at 1250 cm^{-1} is not yet assigned, but may well contain contributions from $\gamma(C—N^+—CH_3)$ and $\nu(N^+—CH_3)$ since $MV^{+\cdot}$ has one fundamental more than $BP^{-\cdot}$ below 1700 cm^{-1}.

Type 3 modes are either overtones or originate in the $MV^{+\cdot}$ dimer (see the following sections). Of the type 4 modes, only that at 282 cm^{-1} is a fundamental and this contains mainly γ(CCC). The other two bands arise from overtones (see next section).

Using this classification, a simplified picture of the excitation processes in $MV^{+\cdot}$ can be given: (i) the ring C—C stretching movements are mainly involved in the transitions at 395, 605 and ~720 nm; (ii) the movements of the $N^+—CH_3$ group are involved with the transitions in the whole range 350–750 nm, which leads to several constructive and destructive interferences; (iii) γ(CCC) is exclusively coupled with the transitions around 620 nm; (iv) for combination tones and modes belonging to the $MV^{+\cdot}$ dimer, the pattern of behaviour will be described in the next sections.

Overtones and combination bands. Using excitations with λ_{exc} from 350.6 nm up to 676.4 nm, 45 overtones and combination bands of $MV^{+\cdot}$ could be detected. They are assigned to the component fundamentals in Fig. 6 and Table 5. Comparing Fig. 6, which represents the qualitative excitation profiles of the overtones and combination bands, with the excitation profiles of the fundamentals given in Fig. 5, the following fact is quite easily seen. With two exceptions, the 32 overtones and combination bands in Fig. 6 appear only in those regions of λ_{exc} where all the component fundamentals also show considerable resonance enhancement. But, *vice versa*, resonance enhancement of the component fundamentals in a specific wavelength range does not necessarily lead to enhancement of the overtones and combination bands in this range.

A comparison between expected and measured wavenumbers of overtones in Fig. 6 shows that the potential surface for most of the modes may be taken as harmonic. The second overtone of the 1662 cm^{-1} band, which is expected at 4986 cm^{-1}, lies at 4984 cm^{-1}, which is well within the experimental error.

Resonance Raman spectra of concentrated $MV^{+\cdot}$ solutions. The RR spectra of concentrated ($\sim 3\times10^{-3}$ M) aqueous $MV^{+\cdot}$ solutions in the fundamental region showed some completely new bands and other bands whose intensities had increased by a larger factor than the concentration increase in going from the original dilute ($\leq 3.9\times10^{-4}$ M) solutions. These bands, which we assign to the $MV^{+\cdot}$ dimer, are found at the following wavenumbers: 664, 1028, 1188, 1340, 1512, 1534, 1604 and 2538 cm^{-1} (see Figs 7 and 8). The combination tone at 2538 cm^{-1}, composed of the 1028 and 1512 cm^{-1} fundamentals, showed much higher relative intensity in spectra from the concentrated $MV^{+\cdot}$ solutions. This confirms the composition of the overtone and also the assignment of the 1512 cm^{-1} band to the dimer. On the other hand, it infers that the band at 1028 cm^{-1} also belongs to the dimer, since otherwise no combination tone could exist. However, the 1028 cm^{-1} dimer band has to be much less intense than the corresponding band of the monomer, since no drastic relative intensity changes occur for this band when changing the solution concentration (see Fig. 7).

A further confirmation that the bands listed arise from the $MV^{+\cdot}$ dimer is the excitation wavelength region, λ_{exc} = 450–520 nm, in which these bands could most easily be detected (see p. 40 above). This range coincides with a maximum absorption of $MV^{+\cdot}$ dimer at −100 °C in methanol.[56] The other peak of the $MV^{+\cdot}$ dimer absorption is at 355 nm.[56] As Fig. 3 shows, the dimer band at 1512 cm^{-1} could indeed be seen very well even in the dilute solution with λ_{exc} = 350.6 nm.

© Heyden & Son Ltd, 1982

RR studies also have been reported for the free radical dimers of *p*-phenylenediamine cation,[57,58] *p*-benzosemiquinone anion,[59] chloranil anion,[60] tetracyanoethylene anion,[61] some Würster's cations,[62] several benzidine cations[63] and *p*-diphenylosemiquinone.[63] In each case, low wavenumber bands in the range 100–200 cm^{-1} were observed. These have been assigned to intermolecular stretching vibrations[57–63] for which force constants of ~1 mdyn $Å^{-1}$ could be calculated.[57,62,63]

No such bands were observed in this investigation of $(MV^{+\cdot})_2$, probably due to unfavourable resonance conditions. The absorption spectra of the radicals discussed in Refs 57–59 and 64 all show intense absorptions at ~300 nm and weaker and broader ones at ~450 nm. Upon dimerization, in each case both bands shift to slightly shorter wavelengths and a new band appears at ~600 nm. It is only by excitation within this long wavelength band that the intermolecular stretching bands have been observed. The long wavelength absorption band has been assigned to charge transfer within the dimers which were assumed themselves to be charge transfer complexes.[64,65] This assumption has recently been questioned[62] and a real, although weak, covalent bond between the two parts of a radical dimer is assumed to exist. This prediction has already been made for $(MV^{+\cdot})_2$ in Ref. 22. Except for a large red shift, the absorption spectra of $MV^{+\cdot}$ and $(MV^{+\cdot})_2$ look very similar[22,56] to those of the other radicals and their dimers reported in Refs 57–59 and 64, with the extra dimer band occurring at ~870 nm.[22] In order to see the low wavenumber intermolecular stretching band, excitation of the RR spectrum at ~870 nm would, therefore, be necessary for $(MV^{+\cdot})_2$.

The dimer bands reported here probably all belong to ring vibrations. They are shifted by −20 cm^{-1} on average as compared with the monomer, assuming the wavenumber correlations 682/664, 1028/1028, 1212/1188, 1356/1340, 1534/1512, —/1534, 1662/1604 for $MV^{+\cdot}/(MV^{+\cdot})_2$. Similar shifts in vibrational wavenumbers were observed for the pair $bpy/bpy^{-\cdot}$,[45] suggesting that the RR bands ascribed to $(MV^{+\cdot})_2$ may originate from a species slightly more reduced than $MV^{+\cdot}$ itself. The question of how the exact electronic structure of $(MV^{+\cdot})_2$ should be depicted can, however, not be answered at the present stage.

Acknowledgements

Financial support from the British Science Research Council, NATO and the Swiss National Foundation (M.F.) are gratefully acknowledged. We should also like to thank Dr H. F. Shurvell from Queen's University, Canada, for helpful discussions and Dr J. Corset for the sight of his electrochemically generated $MV^{+\cdot}$ spectra before publication.

REFERENCES

1. J. A. Farrington, M. Ebert and E. J. Land, *J. Chem. Soc. Faraday Trans. 1*, **74**, 665 (1978).
2. K. Kalyanasundaram, J. Kiwi and M. Grätzel, *Helv. Chim. Acta* **61**, 2720 (1978).
3. A. Moradpour, E. Amouyal, P. Keller and H. Kagan, *Nouv. J. Chim.* **2**, 547 (1978).
4. H. D. Abruña, A. Y. Teng, G. J. Samuels and T. J. Meyer, *J. Am. Chem. Soc.* **101**, 6745 (1979).
5. M. Kirch, J. M. Lehn and J. P. Sauvage, *Helv. Chim. Acta* **62**, 1345 (1979).
6. D. C. Bookbinder, N. S. Lewis, M. G. Bradley, A. B. Bocarsly and M. S. Wrighton, *J. Am. Chem. Soc.* **101**, 7721 (1979).
7. K. Kalyanasundaram and M. Grätzel, *Angew. Chem. Int. Ed. Engl.* **18**, 701 (1979).
8. J. Kiwi, E. Borgarello, E. Pelizzetti, M. Visca and M. Grätzel, *Angew. Chem. Int. Ed. Engl.* **19**, 646 (1980).
9. R. J. Crutchley and A. B. P. Lever, *J. Am. Chem. Soc.* **102**, 7128 (1980).
10. P. B. Sweetser, *Anal. Chem.* **39**, 979 (1967).
11. J. S. Bellin, R. Alexander and R. D. Mahoney, *Photochem. Photobiol.* **17**, 17 (1973).
12. R. C. Young, T. J. Meyer and D. G. Whitten, *J. Am. Chem. Soc.* **98**, 286 (1976).
13. K. P. Seefeld, D. Möbius and H. Kuhn, *Helv. Chim. Acta* **60**, 2608 (1977).
14. I. Okura and N. K. Thuan, *J. Chem. Soc. Commun.* 84 (1980).
15. J. R. Darwent, K. Kalyanasundaram and G. Porter, *Proc. 3rd Int. Conf. Photochem. Conversion Storage Sol. Energy*, p. 3 (1980).
16. T. Tanno, D. Wöhrle, M. Kaneko and A. Yamada, *Proc. 3rd Int. Conf. Photochem. Conversion Storage Sol. Energy*, p. 161 (1980).
17. M. Forster and R. E. Hester, *Proc. 3rd Int. Conf. Photochem. Conversion Storage Sol. Energy*, p. 189 (1980).
18. T. Kawai, K. Tanimura and T. Sakata, *Chem. Lett.* 137 (1979).
19. J. Kiwi and M. Grätzel, *J. Am. Chem. Soc.* **101**, 7214 (1979).
20. P. Keller and A. Moradpour, *J. Am. Chem. Soc.* **102**, 7193 (1980).
21. A. Benchenane, L. Bernard and T. Théophanides, *J. Raman Spectrosc.* **2**, 543 (1974).
22. E. M. Kosower and J. L. Cotter, *J. Am. Chem. Soc.* **86**, 5524 (1964).
23. W. Kiefer and H. J. Bernstein, *Appl. Spectrosc.* **25**, 500 (1971).
24. R. J. H. Clark, in *Advances in Infrared and Raman Spectroscopy*, ed. by R. J. H. Clark and R. E. Hester, Vol. 1, p. 143, Heyden, London (1975).
25. D. A. Long, *Raman Spectroscopy*, p. 134, McGraw-Hill, New York (1977).
26. J. P. Porchet and Hs. H. Günthard, *J. Phys. E* **3**, 261 (1970).
27. A. C. Albrecht and M. C. Hutley, *J. Chem. Phys.* **55**, 4438 (1971).
28. W. M. Schwarz Jr, Ph.D. thesis, University of Wisconsin (1961).
29. G. Zerbi and S. Sandroni, *Spectrochim. Acta Part A* **24**, 511 (1968).
30. S. Yamaguchi, N. Yoshimizu and S. Maeda, *J. Phys. Chem.* **82**, 1078 (1978).
31. C. Takahashi and S. Maeda, *Chem. Phys. Lett.* **24**, 584 (1974).
32. R. N. Jones, *NRCC Bull.* **12**, 9 (1968).
33. J. H. Russell and S. C. Wallwork, *Acta Crystallogr. Sect. B* **28**, 1527 (1972).
34. C. A. Wulff, *J. Chem. Phys.* **39**, 1227 (1963).
35. A. B. Dempster, D. B. Powell and N. Sheppard, *Spectrochim. Acta Part A* **28**, 373 (1972).
36. R. C. Leech, D. B. Powell and N. Sheppard, *Spectrochim. Acta* **22**, 1 (1966).
37. H. Michelsen, P. Klaeboe, G. Hagen and T. Stroyer-Hansen, *Acta Chem. Scand.* **26**, 1576 (1972).
38. E. Spinner, *Aust. J. Chem.* **20**, 1805 (1967).
39. M. Raupach, W. W. Emerson and P. G. Slade, *J. Colloid Interface Sci.* **69**, 398 (1979).
40. G. Zerbi and S. Sandroni, *Spectrochim. Acta Part A* **24**, 483 (1968).
41. H. Kuwata, *J. Sci. Hiroshima Univ. Ser. A-2* **32**, 87 (1968).
42. R. M. Barrett and D. Steele, *J. Mol. Struct.* **11**, 105 (1972).
43. C. Mahon and W. L. Reynolds, *Inorg. Chem.* **6**, 1927 (1967).
44. C. D. Schmulbach, C. C. Hinckley and D. Wasmund, *J. Am. Chem. Soc.* **90**, 6600 (1968).
45. E. König and E. Lindner, *Spectrochim. Acta Part A* **28**, 1393 (1972).

© Heyden & Son Ltd, 1982

46. R. Zahradník and P. Čársky, *J. Phys. Chem.* **74**, 1240 (1970).
47. S. Hünig, D. Scheutzow, P. Čársky and R. Zahradník, *J. Phys. Chem.* **75**, 335 (1971).
48. R. E. Hester and K. P. J. Williams, *J. Chem. Soc. Faraday Trans. 2* **77**, 541 (1981).
49. G. Varsányi, *Assignments for Vibrational Spectra of Seven Hundred Benzene Derivatives*, p. 104. A. Hilger, London (1974).
50. A. G. Evans, R. E. Alford and N. H. Rees, *J. Chem. Soc. Perkin Trans. 2* 1831 (1979).
51. A. G. Evans, J. C. Evans and M. W. Baker, *J. Am. Chem. Soc.* **99**, 5882 (1977).
52. J. A. Shelnutt, D. C. O'Shea, N. T. Yu, L. D. Cheung and R. H. Felton, *J. Chem. Phys.* **64**, 1156 (1976).
53. J. A. Shelnutt, L. D. Cheung, R. C. C. Chang, N. T. Yu and R. H. Felton, *J. Chem. Phys.* **66**, 3387 (1977).
54. J. A. Shelnutt and D. C. O'Shea, *J. Chem. Phys.* **69**, 5361 (1978).
55. M. Pawlikowski and M. Z. Zgierski, *Proc. 7th Int. Conf. Raman Spectrosc.*, p. 310 (1980).
56. A. G. Evans, N. K. Dodson and N. H. Rees, *J. Chem. Soc. Perkin Trans 2* 859 (1976).
57. K. Yokoyama and S. Maeda, *Chem. Phys. Lett.* **48**, 59 (1977).
58. E. E. Ernstbrunner, R. B. Girling, W. E. L. Grossman, E. Mayer, K. P. J. Williams and R. E. Hester, *J. Raman Spectrosc.* **10**, 161 (1981).
59. S. Yamaguchi, K. Yokoyama and S. Maeda, *Bull. Chem. Soc. Jpn* **51**, 3193 (1978).
60. S. Matsuzaki, T. Mitsuishi, C. Etoh and K. Toyoda, *Chem. Lett.* 1417 (1979).
61. K. Yokoyama, S. Maeda, C. Etoh, S. Matusuzaki and K. Toyoda, *Bull. Chem. Soc. Jpn* **53**, 36 (1980).
62. K. Yokoyama, Y. Tajima, M. Tahara and S. Maeda, *Bull. Chem. Soc. Jpn* **53**, 2489 (1980).
63. K. P. J. Williams, Ph.D. Thesis, University of York (1981).
64. K. Kimura, H. Yamada and H. Tsubomura, *J. Chem. Phys.* **48**, 440 (1968).
65. N. Sakai, I. Shirotani and S. Minomura, *Bull. Chem. Soc. Jpn* **44**, 675 (1971).

Received 26 March 1981

© Heyden & Son Ltd, 1982

© Heyden & Son Ltd, 1982